

# Influence of the Graphite Absorber During Laser Surface Hardening

Tomaž Kek - Janez Grum\*

University of Ljubljana, Faculty of Mechanical Engineering, Slovenia

*The paper presents the results of the research of a laser surface hardening process applied to the C45E steel with graphite absorber coating on specimen surfaces. The evaluation of the laser surface hardening process was performed by measuring the IR radiation from the interaction spot. The results confirmed a strong correlation between the IR radiation voltage signal and the dimensions of microstructural changes occurring in the laser surface hardening steel.*

*Changes of the absorbing coating thickness produced changes of the absorptivity of the laser beam, which was confirmed by measurements of the depth and width of hardened traces. For laser surface hardening the optimum coating thickness of a graphite absorber was determined. A factorial analysis and a method of orthogonal polynomials were used to determine response surfaces for the voltage signal of IR radiation the depth and width of the hardened trace achieved. Absorptivity difference between various graphite absorber coating thicknesses was evaluated based on the Ashby-Shercliff model.*

©2010 Journal of Mechanical Engineering. All rights reserved.

**Keywords:** laser surface hardening, IR radiation, IR photodiode, steel C45E, absorption, interaction

## 0 INTRODUCTION

Laser technology is a very young technology, which has reached the age of 40 years [1]. The unusual properties of laser light can be used in a variety of ways for industrial applications. A wide variety of inspection and measurement procedures may be accomplished using lasers [2] and [3]. Also for lots of engineering applications the laser can be regarded as a device for producing a finely controllable energy beam, which, in contact with a material, generates considerable heat. The laser beam is becoming a very important engineering tool for cutting, welding and heat treatment.

For surface treatment of metals, CO<sub>2</sub> lasers are most often used as they can provide high powers of the laser beam. CO<sub>2</sub> laser-beam light, however, is characterized by a comparatively long wavelength, 10.6 μm, which in the interaction with the steel surface at the ambient temperature can ensure only up to 5% of the energy absorbed (polished surface) [4] and [5]. A higher efficiency of laser treatment, however, can be achieved by increasing the laser-beam absorption; therefore, absorbing coatings are frequently used in practical applications.

For the control of the laser heat treatment processes, mainly the signals of IR radiation,

captured from the interaction spot, and the acoustic emission generated during the process itself, are suitable [6] and [7]. IR radiation is generated by the heated solid, liquid, and gas phases at the interaction spot. When a laser beam passes across an absorbing coating on the workpiece surface, the absorber will burn off and the IR radiation will increase. The intensity of the IR radiation is not directly related to the temperature obtained at the workpiece surface on the basis of which the achieved depth of the hardened trace in the steel could be calculated. Nevertheless, the results have shown that there is a strong correlation between the intensity of the IR radiation generated at the interaction spot and the depth and width of the hardened trace when absorbing coating is applied.

The surface temperature in laser surface hardening is mainly the result of the energy balance between the amount of the energy supplied by the laser beam and the amount of conducted energy into material. Energy conduction in the three-dimensional body can be evaluated by the following equation:

$$\rho c_p \frac{\partial T}{\partial t} = \frac{\partial}{\partial x} \left( K \frac{\partial T}{\partial x} \right) + \frac{\partial}{\partial y} \left( K \frac{\partial T}{\partial y} \right) + \frac{\partial}{\partial z} \left( K \frac{\partial T}{\partial z} \right) + Q_v(x, y, z, t) \quad (1)$$

where  $\rho$  [kg/m<sup>3</sup>] is density,  $K$  [W/mK] is thermal conductivity,  $c_p$  [J/kgK] is specific heat capacity,  $Q_V$  [W/m<sup>3</sup>] is heat supplied to a sample in a unit of time per unit of volume,  $T$  [°C] is temperature,  $t$  [s] is time,  $\alpha$  [m<sup>2</sup>/s] is thermal diffusivity.

The Eq. (1) can be applied to a homogeneous and isotropic body as:

$$\nabla^2 T - \frac{1}{\alpha} \frac{\partial T}{\partial t} = - \frac{Q_V(x, y, z, t)}{K}.$$

Taking the abovementioned equation into account, Ashby and Shercliff [8] developed a frequently used temperature distribution model in the workpiece during the laser beam passage, with a Gaussian distribution. An analytical solution for material temperature  $T(y, z, t)$  at a specific transversal distance  $y$  from the laser-beam centre, at specific depth  $z$  and in a certain time period  $t$  is represented by the following equation:

$$T(y, z, t) = T_0 + \frac{AP}{2\pi v K (t(t+t_0))^{1/2}} e^{-\frac{1}{4\alpha} \left( \frac{(z+z_0)^2}{t} + \frac{y^2}{t+t_0} \right)}. \quad (2)$$

This analytical solution is based on the assumption that specific heat capacity  $c_p$ , thermal conductivity  $K$  and thermal diffusivity  $D$  are constants and that the latent heat of the phase transition  $\alpha\gamma$  is negligible.

The value  $t_0$  is a time period within which the heat is diffused across the distance equal to the laser-beam radius.

$$t_0 = \frac{r_b^2}{4\alpha}.$$

The value  $z_0$  is the distance covered by heat diffusion within a time period of  $2r_b/v$ . This constant is used to constrain the surface temperature to finite value. The constant  $C_1$  depends on the material treated.  $z_0$  is calculated using the following equation:

$$z_0^2 = \frac{\pi\alpha r_b}{2C_1 e v}.$$

## 1 EXPERIMENTAL PROCEDURE

The experiments on laser surface hardening were conducted using an industrial CO<sub>2</sub> laser, Spectra Physics 820. The laser beam shows a Gaussian TEM<sub>00</sub> mode. For testing, flat specimens made from C45E (SIST EN 10027-1) steel were used. This plain carbon hypo-eutectic

steel is, namely, suitable also for laser surface hardening. In all the tests conducted laser surface transformation hardening was performed under conditions which caused no melting of the thin surface layer.

In the study, specimens of 200 x 45 x 12 mm in size were used. The specimen surface was ground to a roughness of  $Ra = 1.6 \mu\text{m}$ . Graphite absorber was deposited (sprayed with air as assistant gas) in different thicknesses  $\delta = 10, 40,$  and  $70 \mu\text{m}$  on the specimens. The thickness of graphite absorber deposition was measured with weighting of thin steel sheet reference specimen. The deposition of graphite absorber on reference specimens was made together with an individual specimen (200 x 45 x 12 mm). Twelve laser-hardened traces were produced in the transverse specimen direction on each flat specimen. The distance and treatment time between the individual traces on the specimen was large enough not to allow perceivable thermal influence between the adjacent traces. The focal length of the lens used was  $f = 127 \text{ mm}$  and a defocusing degree  $z_s = 31 \text{ mm}$ . The laser-beam diameter at the specimen surface was  $D_b = 3.9 \text{ mm}$ . The laser-beam power was  $P = 900 \text{ W}$ . Three laser-hardened traces were produced with each absorbing coating thickness and with each travel speed:  $v_{b,1} = 220 \text{ mm/min}$  ( $E_{d,1} = P/(v_1 D_b) = 63 \text{ J/mm}^2$ ),  $v_{b,2} = 280 \text{ mm/min}$  ( $E_{d,2} = 49 \text{ J/mm}^2$ ),  $v_{b,3} = 340 \text{ mm/min}$  ( $E_{d,3} = 41 \text{ J/mm}^2$ ) in  $v_{b,4} = 400 \text{ mm/min}$  ( $E_{d,4} = 35 \text{ J/mm}^2$ ). In the treatment no shielding gas was used.

The IR electromagnetic radiation from the interaction spot was captured with the photodiode (Fig. 1), which was at  $r = 10 \text{ cm}$  from the interaction spot. Photodiode permitted monitoring of the electromagnetic radiation in the wavelength range between 0.4 and 1  $\mu\text{m}$  with the highest responsivity of the photodiode at 0.85  $\mu\text{m}$ . The active area of the photodiode equalled 1 mm<sup>2</sup>. The mean values of the voltage signal of IR radiation  $U$  were determined in a time span of 0.3 s.

## 2 EXPERIMENTAL RESULTS

### 2.1 The IR Radiation Voltage Signal

In the analysis of the data measured in laser surface hardening, the factorial analysis was used. Factorial analysis is the most efficient in the experiments in which the influence of two or

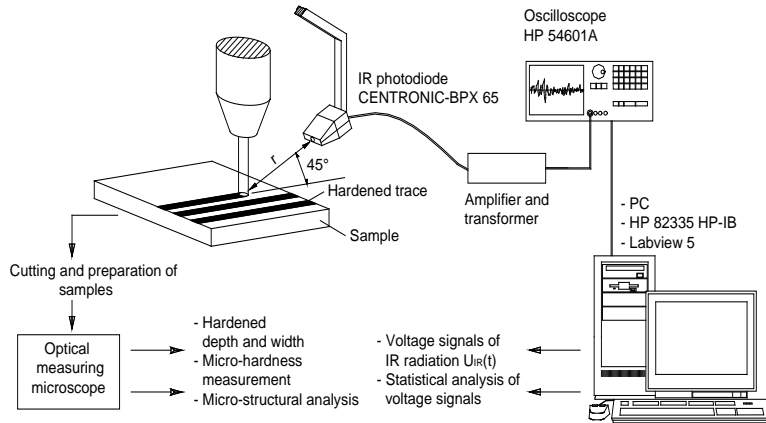


Fig. 1. Experimental setup for capturing and evaluation of voltage signal of IR radiation and for measuring hardened traces

more factors is studied [9]. The influence of a factor is defined as a change in response with a change in the level of a factor.

The factorial analysis is advantageous primarily when there are interactions between the factors and when it permits an evaluation of the influences of the individual factors with different levels of other factors. This ensures correct conclusions over the range chosen of laser-hardening conditions.

Table 1. Extended analysis of variance

Source of variation	Sum of squares $SS_i$ [db <sup>2</sup> ]	Degrees of freedom $v_i$	Mean square $MS_i$ [db <sup>2</sup> ]	$F_0$	$F_{0,05,v_{i,24}}$
Absorber	0.04242	2	0.02121	100.44	3.40
$D_L$	0.03832	1	0.03832	181.46	4.26
$D_Q$	0.00410	1	0.00410	19.41	4.26
Travel speed	0.19960	3	0.06653	315.04	3.01
$V_L$	0.19807	1	0.19807	937.90	4.26
$V_Q$	0.00151	1	0.00151	7.16	4.26
$V_C$	0.00001	1	0.00001	0.05	4.26
Interaction	0.00771	6	0.00128	6.08	2.51
$DV_{LxL}$	0.00616	1	0.00616	29.18	4.26
$DV_{LxQ}$	0.00103	1	0.00103	4.89	4.26
$DV_{LxC}$	0.00005	1	0.00005	0.26	4.26
$DV_{QxL}$	0.00037	1	0.00037	1.77	4.26
$DV_{QxQ}$	0.00002	1	0.00002	0.08	4.26
$DV_{QxC}$	0.00007	1	0.00007	0.33	4.26
Error	0.00507	24	0.00021		
Total	0.25480	35			

Indices  $L, Q, K$  – linear, quadratic and cubic effects of absorbing coating thickness designated  $D$  and of cutting speed designated  $V$  i.e. their interaction  $DV$ . A more detailed definition can be found in [9].

The results of the analysis of the variance of the voltage signal of IR radiation are given in Table 1. The experimental procedure was performed with three repetitions with the given combinations of the processing conditions. The influence of the absorbing coating thickness and cutting speed on the voltage signal of IR radiation was analysed. The  $F_0$  test statistics representing a ratio of mean squares and which belongs to the Snedecor distribution  $F$  is given in Table 1.

A significant influence on the IR radiation voltage signal was determined with reference to the factorial analysis of the experimental data. These influences include linear  $D_L$  and square  $D_Q$  influences of the absorbing coating thickness, linear  $V_L$  and square  $V_Q$  influences of travel speed, and the interaction influences,  $DV_{LxL}$  and  $DV_{LxQ}$ . Significant influences are indicated as shaded lines in Table 1. Taking into account these significant influences on the voltage signal, the method of orthogonal polynomials was used to develop an approximation polynomial (3) of the 3D response surface (Fig. 2) for the treatment conditions used:

$$U = -0.122 + 2.51 \cdot 10^{-4} \delta - 2.51 \cdot 10^{-5} \delta^2 + 0.001v + 6.28 \cdot 10^{-7} v^2 + 2.97 \cdot 10^{-5} \delta v - 6.07 \cdot 10^{-8} \delta v^2. \quad (3)$$

Based on the approximation polynomial, it can be estimated that the voltage signal of the greatest intensity will be within the studied processing parameters area at  $\delta = 50 \mu\text{m}$  and  $v = 400 \text{ mm/min}$ .

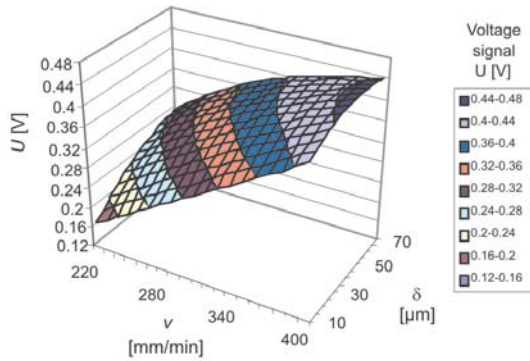


Fig. 2. Three-dimensional response surface of the IR voltage signal

A comparison between the values  $U$  calculated by using the approximation polynomial obtained with equation (3) and the mean values  $\bar{U}_{ij}$  of the voltage signals measured under the selected laser surface hardening condition is given in Fig. 3. The value of  $R^2$  of the measured values of the IR radiation voltage signal and the approximation polynomial equals 0.98.

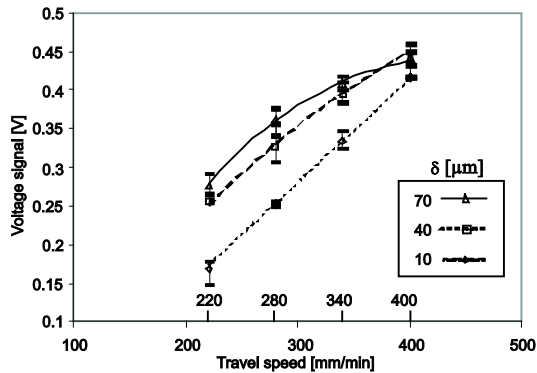


Fig. 3. The graph of the approximation polynomial (3) and the mean values  $U$  with the ranges of the measured values of the IR radiation voltage signals

When the laser beam passes across the specimen surface to which an absorbing coating has been applied, the temperature of the absorber immediately greatly increases. This may cause evaporation and burn-off of the absorber. The absorber's burn-off is related to intense exothermal oxidation processes at the interaction spot. The heated microscopic graphite particles, hot gases (mainly  $CO_2$ ), and the heated specimen surface at the interaction spot emit the IR radiation.

Based on the measured magnitude of the voltage signal of IR radiation it is estimated that with thicker coatings a larger quantity of the absorber burns-off. Similarly, an increase in the travel speed of the laser beam results in a larger quantity of absorber burnt-off per unit of time.

The IR voltage signal increases with an increase in the energy supplied to the interaction spot at the same laser travel speed (Fig. 4).

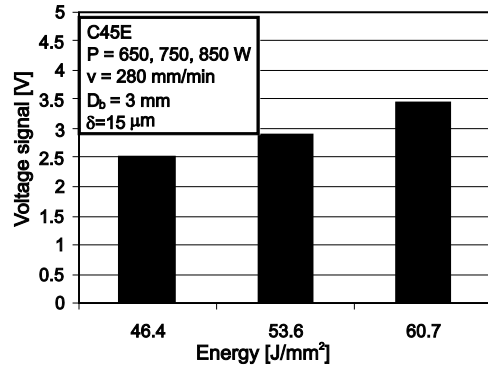


Fig. 4. IR radiation voltage signal  $U$  in laser surface hardening

Higher laser beam power increases temperatures at the interaction spot and causes a stronger burn-off of the absorber. The IR voltage signal is also affected by the type and flow of protective gas, as well as by the position and distance of the photodiode from the interaction spot. The burn-off process differed according to the type of the absorber used due to the absorbers' different ingredients and structure. This affects the IR radiation emitted from the interaction spot and, consequently, the measured IR radiation voltage signal.

In this specific case of laser surface hardening with the use of a graphite absorber, no significant difference was found in the IR radiation voltage signal power spectra with different laser beam travel speeds.

### 2.2 Size of the Microstructure Changes

In spite of the burn-off of the graphite absorber, its presence produces an increased absorptivity at the interaction spot. It should be considered, however, that the absorptivity of the laser beam is affected also by the coating thickness. This shows (Fig. 5a) in different depths and widths of the hardened trace obtained with

the same travel speed of the laser beam across the specimen surface.

Courtney showed a linear dependency between the parameter  $P/\sqrt{D_b v}$  and the depth of the hardened trace in laser surface hardening. The linear dependency for the measured values is given in Fig. 5b. The measured values follow regression lines nicely which supports linear dependency also in the use of the absorber.

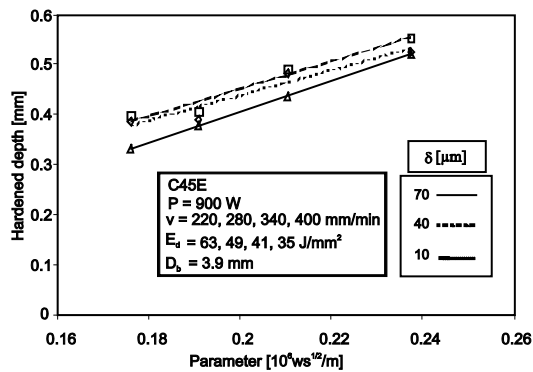
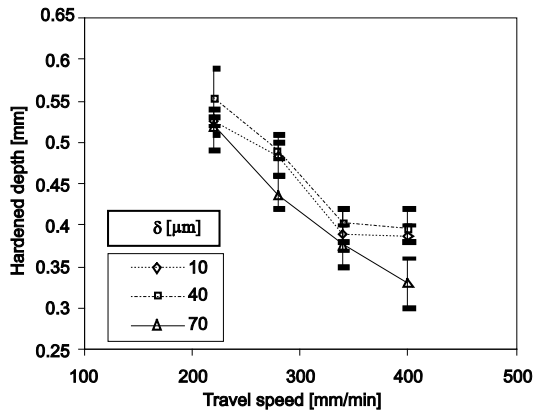


Fig. 5. a) Influence of travel speed and absorbing thickness on the depth of the hardened trace, b) Influence of the parameter  $P/\sqrt{D_b v}$  and the absorber A thickness on the depth of the hardened trace

A contour plot in Fig. 6 indicates the depths of the hardened trace based on the approximation polynomial. The value of R2 for the measured values of the hardened depth and the approximation polynomial equals 0.91. A similar influence of the travel speed and absorber thickness was established also for the hardened width (Fig. 7). The value R2 for the measured

values of the hardened width and the approximation polynomial equals 0.89.

The amount of the energy supplied by the laser beam to the treated steel is higher with lower travel speeds, which makes the hardened area of the steel's surface layer wider and deeper. Higher temperatures are achieved and time periods of maintaining steel at high temperatures are extended. This enables a more homogeneous carbon distribution in the crystal grains which is reflected in a more uniform hardness distribution across the hardened trace.

From the written polynomial of the response surface for the depth of the hardened trace it follows that the greatest depths of the hardened trace can be expected with the coating thickness of the graphite absorber  $\delta_{opt} = 32 \mu\text{m}$ . For the given experiment, this thickness may be called the optimum coating thickness of the graphite absorber. The optimum coating thickness determined by means of the approximation polynomial for the hardened-trace width was very similar at  $35 \mu\text{m}$ .

The experiments conducted indicate a relationship between the voltage signal of IR radiation and the hardened-trace depth, which is shown in Fig. 8. It can be stated that with a high value of the voltage signal of IR radiation, the depth and width of the hardened trace are smaller, and vice versa.

To exclude the possibility of the correlation between the data given above being merely of an apparent nature, *t* test is used. The calculation of the *t* value for the hardened depth and the number of specimen elements  $n = 36$  is as follows:

$$t = r_{xy} \sqrt{\frac{n-2}{1-r_{xy}^2}} = -8.887.$$

At the Student's *t* distribution, with  $n - 2 = 34$  degrees of freedom and  $\alpha = 0.001$ , the critical area is defined with the value  $t_{0.0005,34} = \pm 3.608$ . Based on calculated *t* value, it may be concluded that there is a correlation between the IR radiation voltage signal and the hardened depth and that it is highly unlikely that it is coincidental. Value *t* for the correlation between the IR radiation voltage signal and the hardened width  $t = -7.635$ .

Correlation coefficients  $r_{xy}$  between the measured values of the IR radiation voltage signal and the measured hardened depths and widths are

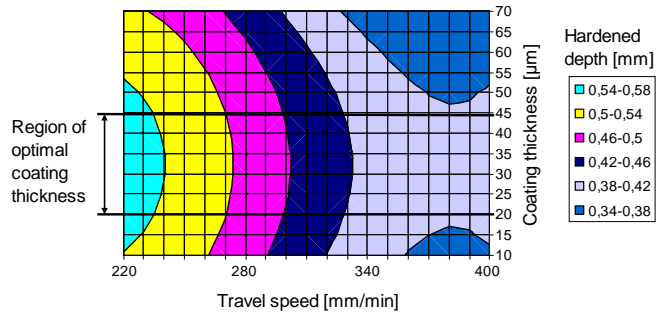


Fig. 6. Influence of travel speed and absorber thickness on the hardened depth

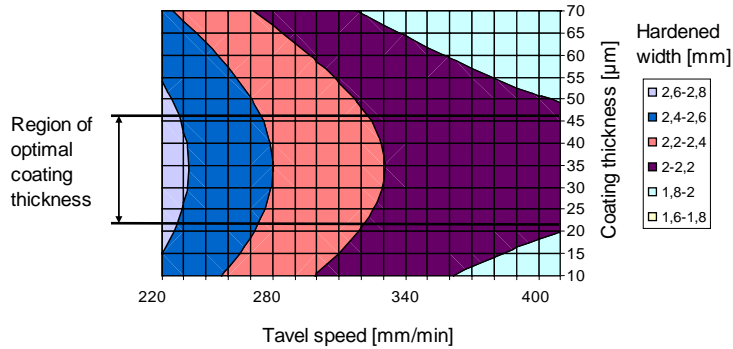


Fig. 7. Influence of travel speed and absorber thickness on the hardened width

given in Table 2. along with the correlation coefficients between the IR radiation voltage signal values calculated on the basis of the approximation polynomial (3) and the measured geometrical parameters of the microstructure changes. It may be concluded that the correlation between the voltage signal and the depth and width of the hardened trace with each individual absorber thickness is good.

### 2.3 Influence of the Absorber on Absorptivity

Heat is conducted through the absorber to the specimen surface. Taking into account the thinning of the absorber due to its burn-off and evaporation, the optimum absorber thickness is a combination of the absorber thickness within which the absorption of the laser-beam light occurs and the heat conductivity of the absorber. With an absorbing coating thickness smaller than the optimum one, a premature elimination of the absorber in the interaction with the laser beam occurs. A portion of the laser beam therefore, falls on the specimen surface with no absorbing coating. Consequently, the quantity of the laser-beam energy absorbed by the specimen is smaller.

With a coating thickness thicker than the optimum one, only a portion of the absorber burns-off when the laser beam passes over the surface. The remaining portion may present an obstacle to the conduction of heat energy through the absorber to the steel surface. With the optimum absorbing coating thickness, the laser beam is falling during the whole interaction time on the absorber and efficient transformation of the laser-beam energy into the heat energy accumulated in the specimen is obtained.

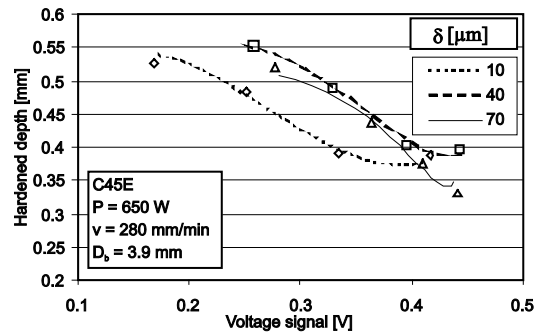


Fig. 8. Correlation between the IR radiation voltage signal and the hardened depth based on approximation polynomials (curves) and mean values of measured ha. depths (signs)

Table 2. Correlation coefficients  $r_{xy}$  between the values of the IR radiation voltage signal  $U$  and the measured depths  $d$  and widths  $w$  of the hardened trace

Correlation coefficient $r_{xy}$	Hardened depth $d$				Hardened width $w$			
	Total	10 $\mu\text{m}$	40 $\mu\text{m}$	70 $\mu\text{m}$	Total	10 $\mu\text{m}$	40 $\mu\text{m}$	70 $\mu\text{m}$
Measured value $U$	-0.84	-0.93	-0.93	-0.92	-0.70	-0.89	-0.93	-0.90
$U$ calculated by using the approximation polynomial	-0.84	-0.90	-0.93	-0.95	-0.81	-0.92	-0.93	-0.95

It can be expected that the optimal absorber thickness will be smaller with higher travel speeds and bigger with lower travel speeds [10]. In our experiment, this phenomenon was not sufficiently evident to be detected through significant interaction between absorber thickness and travel speed influence in the factorial analysis of the measured values of the depth of the hardened trace (with  $\alpha = 0.05$ ). It can be assumed that in our research, by extending the absorber thickness range and/or travel speed, the former would have been confirmed with a significant interaction in the analysis of variance.

Temperature values calculated with Ashby-Shercliff temperature distribution model may be used to evaluate the difference in absorptivity  $A$  that is a consequence of different absorber thicknesses. The measured depths of the hardened trace with different absorber thicknesses are given in Fig. 9 as signs. The depths of the hardened trace determined on the basis of the Ashby-Shercliff model are represented by the curves. The calculated depths of the hardened trace are obtained on the basis of the calculated heating speeds, which determine increased transformation temperature values  $T_{Ac1}$  in a TTA diagram.  $C_1$  is calibrated based on the measurements of absorptivity of graphite coating ( $\delta = 15 \mu\text{m}$ ) with Borik and Giesen calorimetric method together with measurements of thickness of hardened depth on calorimetric specimens.

From Fig. 9 the difference in absorptivity of the graphite absorber coating with different thickness can be estimated. Furthermore, considering a constant absorptivity, the model predicts a more rapid increase of the hardened depth with a decrease in travel speed compared with measured results. This confirms the variability of graphite coating absorptivity with various amounts of the supplied energy to the interaction spot. The amount of the supplied energy is the result of the interaction spot size, laser beam power and travel speed. When using

empirical and analytical temperature distribution models, it is, therefore, imperative to use adjusted absorptivity values for specific laser application with a consideration of laser beam power density and travel speed.

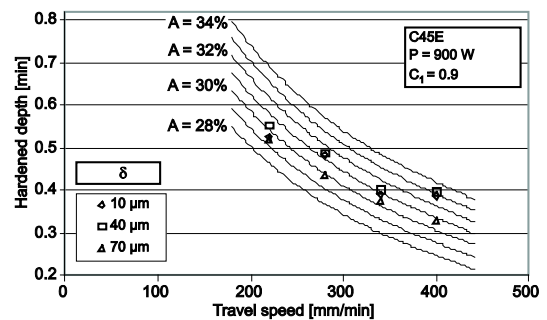


Fig. 9. The measured hardened depths  $d$  (signs) and the calculated hardened depths (curves) in the laser surface hardening of the C45E steel with a graphite absorber

### 3 CONCLUSION

For efficient control of the laser surface hardening process it is of the utmost importance to monitor the thermal phenomena that occurs at the interaction spot between the laser beam and the material. The thermal phenomena at the interaction spot were monitored in the tests carried out with the IR photodiode by measuring the IR radiation voltage signal. The results of the measurements show a good correlation between the IR radiation voltage signal and the size of microstructure changes in the material.

The results of the measurement showed that the absorptivity of the graphite absorber at the specimen surface changes with reference to the absorbing coating thickness. This means that there is an optimum coating thickness depending on the type of the absorber and the laser-hardening conditions. On the basis of the factorial analysis of the measured data and the

determination of the approximation polynomial for the depth and width of the hardened trace. the optimum coating thickness of the graphite absorber was determined. It ranged between 32 and 35  $\mu\text{m}$ .

By using the approximation polynomial. the number of the measurements performed within the predicted area can be reduced. and based on significant influences. the predictability of the response variable among the chosen levels of influential factors can be achieved.

#### 4 REFERENCES

- [1] Radovanović, M. (2006) Some Possibilities for Determining Cutting Data when using Laser Cutting, *Strojniški vestnik - Journal of Mechanical Engineering* vol. 52, no. 10, p. 645-652.
- [2] Bajcar, T., Širok, B., Eberlinc, M. (2009) Quantification of Flow Kinematics Using Computer-Aided, *Strojniški vestnik - Journal of Mechanical Engineering* vol. 55, no. 4, p. 215-223.
- [3] Vukašinović, N., Korošec, M., Duhovnik, J. (2010) The Influence of Surface Topology on the Accuracy of Laser Triangulation Scanning Results, *Strojniški vestnik - Journal of Mechanical Engineering* vol. 56, no. 1, p. 23-30.
- [4] Pantsar, H., Kujanpaa, V. (2006) Effect of oxide layer growth on diode laser beam transformation hardening of steels, *Surface and Coating Technology*, vol. 200, no. 8, p. 2627-2633.
- [5] Grum, J. (2009) Modeling of laser surface Hardening. Gür, C.H., Pan, J. (eds.) *Handbook of Thermal Process Modeling of steels*, CRC Press. Boca Raton, p. 499-626.
- [6] Chryssolouris, G. (1994) Sensors in laser machining, *Annals of the CIRP*, vol. 43, no. 2, p. 513 - 519.
- [7] Steen, W.M. (1996) *Laser material processing*, Springer-Verlag. London, p. 172 - 219.
- [8] Shercliff, H.R., Ashby, M. F. (1991) The prediction of case depth in laser transformation hardening, *Metallurgical Transactions*, vol. 22A, p. 2459-2466.
- [9] Montgomery, D.C. (2000) *Design and analysis of experiments*, John Wiley and Sons, New York, p. 126-289.
- [10] Woo, H.G., Cho, H.S. (1998) Estimation of hardened layer dimensions in laser surface hardening processes with variations of coating thickness, *Surface and Coatings Technology*, vol. 102, p. 205 - 217.